JOURNAL OF SOLID STATE CHEMISTRY **121,** 149–157 (1996)
ARTICLE NO. 0022

Is Electron Paramagnetic Resonance a Valuable Technique for Structural Study of PZG Glass through Recrystallization?

C. Legein,* J. Y. Buzaré,† and C. Jacoboni*

*Laboratoire des Fluorures, URA CNRS 449 and †Equipe de Physique de l'Etat Condensé URA CNRS 807, Faculté des Sciences - Université du Maine, 72017 - Le Mans Cedex, France

Received April 11, 1995; in revised form September 7, 1995; accepted September 13, 1995

Recrystallization of fluoride glasses in the PbF_2–ZnF_2–GaF_3 system (PZG), amorphous GaF_3, and amorphous $PbGaF_5$ have been studied by EPR and XRD. Cr^{3+} and Fe^{3+} are used as EPR probes for PZG glass. Fe^{3+} is the only probe used for the amorphous compounds.

The recrystallization of amorphous GaF_3 leads to well-crystallized rhombohedral GaF_3 (Rh-GaF_3). We have determined the fine structure parameters of Fe^{3+} in Rh–GaF_3 from crystalline powder EPR spectrum simulation. We have then studied the evolution of the fine structure parameters along the recrystallization process. Fine structure parameters of GaF_3:Cr^{3+}, AlF_3, and InF_3 crystalline powders (doped with CrF_3 and FeF_3) were also determined. The superposition model allowed us to compare lattice relaxation around Cr^{3+} and Fe^{3+} probes in these compounds. It shows that Cr^{3+} and Fe^{3+} ions are well adapted for the EPR studies of Ga^{3+}-containing compounds. Amorphous $PbGaF_5$ recrystallization leads to $PbGaF_5$ powder, whose crystallinity, from a local point of view, is not as good as that obtained by direct solid state synthesis. PZG glass recrystallization leads to a mixture of compounds. EPR spectra changes versus heating time treatment are described and interpreted.

INTRODUCTION

In the framework of the study of short-range order in transition metal fluoride glasses (TMFG) (1), the recrystallization of PbF_2–ZnF_2–GaF_3 (PZG) glass (2) was investigated by electron paramagnetic resonance (EPR) using Cr^{3+} and Fe^{3+} probes. Identification of the recrystallized phases was carried out by using X-ray diffraction (XRD). The aim of this study is to try to answer questions such as:

—Is there a crystallized compound representative of local order in TMFG?

—Would it be possible to consider a glass spectrum as a sum of its recrystallization compounds spectra?

According to XRD spectra, the recrystallization of PZG glass leads to a complex mixture of compounds whose proportions vary with time and temperature of heating. Moreover, the structures of PZG glass recrystallization compounds are generally unknown. Therefore, Cr^{3+} or Fe^{3+} fine structure parameters are very difficult to determine especially for low symmetry sites. Heating treatment appears to have significant effects on the spectrum shapes.

We choose to approach the problem by the study of amorphous compounds only containing single (GaF_3) or binary ($PbGaF_5$) fluorides leading to a single compound after recrystallization.

EXPERIMENTAL PROCEDURES

Owing to the fact that fluoride compounds are moisture sensitive, all preparative works were done inside a dry glovebox.

The method used to synthesize PZG glass doped with CrF_3 or FeF_3 was the following: after preliminary mixing, the mixture {(35 PbF_2, 24 ZnF_2, 34 GaF_3, 5 YF_3, 2 AlF_3 mole%) (2) + CrF_3 or FeF_3} was placed in a covered platinum crucible, melted and heated at 800°C, and then cast into a preheated (200°C) mould.

Amorphous GaF_3 and $PbGaF_5$ were obtained by vapor-phase deposition (3, 4). CrF_3 has a vapor pressure lower than FeF_3, GaF_3, and PbF_2; Cr^{3+}-doped amorphous GaF_3 and $PbGaF_5$ are therefore more difficult to obtain. The only EPR probe used for these compounds is thus Fe^{3+}. GaF_3:Fe^{3+} and $PbGaF_5$:Fe^{3+} evaporations were conducted in a 6-cm-diameter pyrex vessel connected to a vacuum system allowing pressure around 10^{-4} mbar. The platinum crucible containing the premelted starting charge (GaF_3 + FeF_3) or (PbF_2 + GaF_3 + FeF_3) was heated with an R.F. coil. The chemical composition of deposited phases was analyzed by induced coupled plasma (ICP).

Recrystallizations were achieved in sealed gold tubes (glasses and $PbGaF_5$) or followed by differential thermal analysis (GaF_3).

AlF_3, GaF_3, and InF_3 crystalline powders doped with CrF_3 or FeF_3 were synthesized by heating the mixture MF_3 + $M'F_3$ (M = Al, Ga, or In and M' = Cr or Fe) at temperatures between 800 and 900°C for 20 to 40 hr in

0022-4596/96 $12.00

TABLE 1
Time and Temperature of Reaction of PZG Glass Recrystallization Compounds

Compound	Temperature (°C)	Time
$PbGaF_5$	630	24 hours
$Pb_3Ga_2F_{12}$	520	24 hours
$Pb_9Ga_2F_{24}$	520	24 hours
Pb_2ZnF_6	510	5 days

sealed platinum tubes in order to obtain homogenous doping. Crystalline powders of $PbGaF_5$, $Pb_3Ga_2F_{12}$, $Pb_9Ga_2F_{24}$ (5), and Pb_2ZnF_6 (6) doped with Fe^{3+} or Cr^{3+} were obtained by solid state reaction of equimolar mixture in sealed platinum tubes. Temperature and time of reaction are listed in Table 1.

The EPR X-band (9.5 GHz) spectra were recorded on a Bruker spectrometer; measurements at variable temperature were achieved by using an Oxford cryostat.

Powder XRD spectra of recrystallized amorphous compounds and glasses were recorded on a diffractometer with back-monochromated CuK radiation monitored by a Siemens Diffrac.At system.

AMORPHOUS GAF_3 RECRYSTALLIZATION

1. The EPR Study of MF_3 Crystalline Powders Doped with CrF_3 or FeF_3: Fine Structure Parameter Determination through EPR Spectra Simulation

AlF_3 (7), GaF_3 (8), and InF_3 (9) crystallize with $R\bar{3}c$ symmetry. The network is built up from corner-shared MF_6 octahedra (Fig. 1). The cationic symmetry site is $\bar{3}$. The relevant spin-Hamiltonian for Fe^{3+} in this case is (10)

$$H = \mu_B \vec{H} \cdot \tilde{g} \cdot \vec{S} + 1/3 b_2^0 O_2^0 + 1/60(b_4^0 O_4^0 + b_4^3 O_4^3) \quad [1]$$

(for Cr^{3+} ions, the fourth-order parameters must be omitted). The $\tilde{g}$ tensor is axial. The relevant O_n^m expressions are given in Table 2.

The line shape calculation procedure has been previously described for TMFG spectra simulation [1].

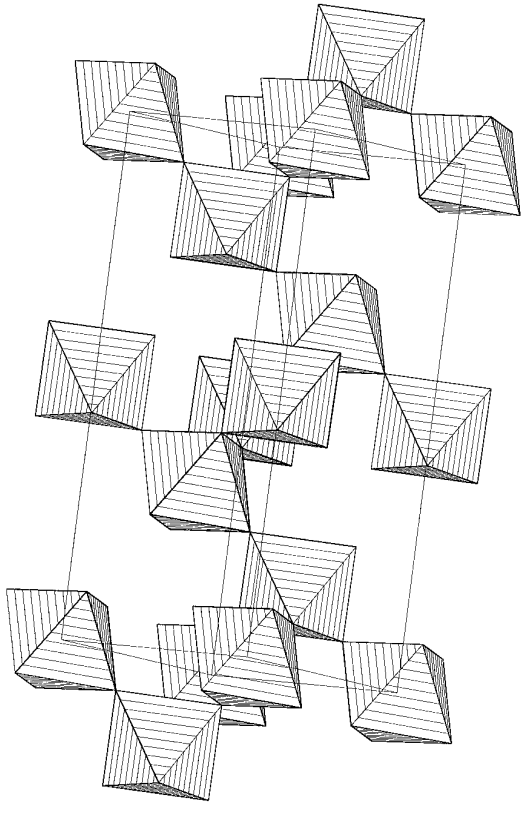

FIG. 1. α-AlF_3 structure; hexagonal cell, $a = 4.9305$ Å, $c = 12.4462$ Å.

For the two ions used as probes, the spectrum anisotropy is mainly related to the fine structure interaction. Thus, one cannot expect any precise determination of the $\tilde{g}$ tensor components. The spin-Hamiltonian parameters, leading to the best agreement between observed and calculated spectra, are given in Table 3 (Cr^{3+} and Fe^{3+}). In this table, one can notice the absence of b_2^2 parameters, which indicates an axial symmetry, and the presence for Fe^{3+} of fourth-order parameters in agreement with the trigonal local symmetry. The powder spectrum simulation allows us to determine the relative b_n^m signs only. The absolute signs were finally determined by using the superposition model which gives the b_2^0 sign (see Section 3).

TABLE 2
O_n^m Expressions

O_n^m
$O_2^0 = 3S_z^2 - S(S+1)$
$O_4^0 = 35S_Z^4 S_x - 30S(S+1)S_Z^2 + 25S_Z^2 - 6S(S+1) + 3S^2(S+1)^2$
$O_4^3 = \frac{1}{4}[S_Z(S_+^3 + S_-^3) + (S_+^3 + S_-^3)S_Z]$

TABLE 3
Cr^{3+} and Fe^{3+} Spin Hamiltonian Parameters ($b_n^m \times 10^4$ cm^{-1})

	Cr^{3+}	Fe^{3+}		
Compound	b_2^0	b_2^0	b_4^0	b_4^3
AlF_3	−360 (±30)	165 (±5)	−12.5 (±1)	325 (±25)
GaF_3	−940 (±10)	190 (±5)	−12.0 (±1)	300 (±25)
InF_3	1350 (±50)	−80 (±5)	25 (±5)	0 (±100)

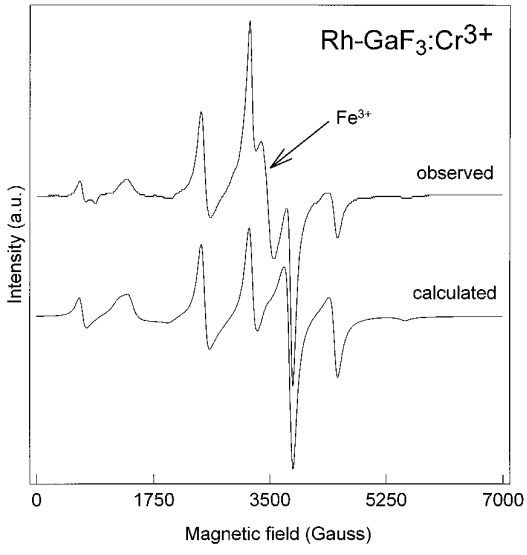

FIG. 2. Observed (2.0 wt% CrF_3; $\nu = 9.45$ GHz) and calculated Cr^{3+} X-band EPR spectra for crystalline powder GaF_3.

—Observed and calculated GaF_3 spectra are shown on Figs. 2 (Cr^{3+}) and 3 (Fe^{3+}); an excellent agreement is obtained.

—Simulation of the $AlF_3:Cr^{3+}$ spectrum leads to well positioned resonances, however, the line shapes (not shown) are not satisfactorily simulated.

—The $InF_3:Cr^{3+}$ EPR spectrum is more difficult to simulate; the resonance positions in the calculated spectrum do not agree with those of the observed spectrum. A previous RAMAN study on MF_3 fluorides has shown that InF_3 structure is questionable (maximal point symmetry: $2/m$ (11)). However, the introduction of a b_2^2 parameter in our calculations did not lead to a better agreement. This shows that further work is needed to determine the InF_3 structure precisely.

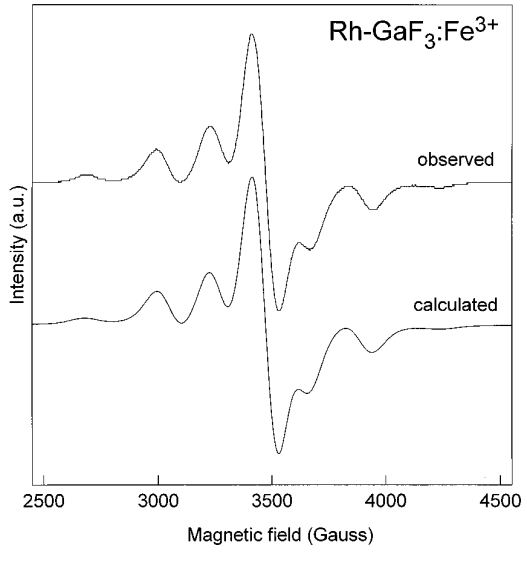

FIG. 3. Observed (1.0 wt% FeF_3; $\nu = 9.66$ GHz) and calculated Fe^{3+} X-band EPR spectra for crystalline powder GaF_3.

2. The Superposition Model (SPM)

The SPM (12) assumes that the spin-Hamiltonian parameters only depend on the local surrounding of the paramagnetic ion through the law.

$$b_n^m = \sum_i b_n(R_i) K_n^m(\theta_i, \varphi_i), \qquad [2]$$

where i runs over the nearest neighbors at coordinates R_i, θ_i, and φ_i. The K_n^m (θ_i, φ_i) terms are angular functions similar to spherical harmonics.

The radial functions $b_n(R_i)$ depend on the probe and ligand type. From several experimental results on fluoroaluminate crystallized compounds, S. Houlbert determined $b_2(R)$ functions for both Cr^{3+} and Fe^{3+} (13) (figures and expression are given in Ref. (1)).

The main point is the slower $b_2(R)$ variation as a function of R for Cr^{3+}. Thus, Fe^{3+} is more sensitive to radial distortions and consequently less sensitive to angular distortions than Cr^{3+}.

For AlF_3 and GaF_3, the cationic symmetry site is $\bar{3}$, the only b_2^m parameter is then

$$b_2^0 = \sum_i b_2(R) \cdot K_2^0(\theta_i, \varphi_i), \qquad [3]$$

with

$$K_2^0 = \frac{1}{2}(3\cos^2\theta - 1). \qquad [4]$$

M–F distances and angle values (θ) between the $\bar{3}$ axis and M–F bonds are given in Table 4. In the MF_6 octahedra, the six M–F distances are equal, thus

$$b_2^0 = 3b_2(R) \cdot (3\cos^2\theta - 1). \qquad [5]$$

The results of the SPM with these $b_2(R)$ functions for Cr^{3+}- and Fe^{3+}-doped AlF_3 and GaF_3 are reported in Table 4. b_2^0 values are calculated under the assumption that the substitution is achieved without any lattice relaxation. θ values are deduced from b_2^0 experimental values by considering an angular relaxation around the paramagnetic probe with a $\bar{3}$ symmetry. We obtained a fine agreement between calculated and experimental fine structure parameters for GaF_3. This may be related to the reduced lattice relaxation around the probes resulting from the closeness of ionic radii of Ga^{3+} and Cr^{3+} or Fe^{3+} (Table 5, Ref. (14)). On the

TABLE 4
Cristallographic M–F Distances (R), Angle Values (θ) between $\bar{3}$ Axis and M–F Bonds, Calculated and Experimental Cr^{3+} and Fe^{3+} b_2^0 Parameters (b_2^0 and $b_2(R) \times 10^4$ cm^{-1}), and θ Values Deduced from Experimental Values for AlF_3 and GaF_3

			Cr^{3+} probe				Fe^{3+} probe			
Compound	R (Å)	θ	b_2 (R)	b_2^0 calc	b_2^0 exp	θ (Cr^{3+})	b_2 (R)	b_2^0 calc	b_2^0 exp	θ (Fe^{3+})
AlF_3	1.797	54.738°	14880	−27.3	−360	54.90°	−4699	8.6	165	54.97°
GaF_3	1.892	55.15°	15913	−974	−940	55.14°	−3536	216	190	55.10°

other hand, the agreement is less satisfying for AlF_3. Thus, it is more advisable, for extracting quantitative description of short-range ordering to have a close-radius EPR probe and host ion. Cr^{3+} and Fe^{3+} are therefore well adapted for $CsZnGaF_6$, amorphous GaF_3, and PZG glass studies (1).

3. Amorphous GaF_3:Fe^{3+} Recrystallization (*Figure* 4)

The amorphous GaF_3:Fe^{3+} EPR spectrum exhibits two main resonances at $g_{eff} = 4.3$ and $g_{eff} = 2.0$. This spectrum is characteristic of Fe^{3+} ions in amorphous fluoride compounds (glasses based on ZrF_4 (15—17) or TMFG (18)). It can be reconstructed with a Czjzek fine-structure parameter distribution (19),

$$P(b_2^0, \lambda) = \frac{1}{(2\pi)^{1/2}\sigma^d}(b_2^0)^{d-1}\lambda\left(1 - \frac{\lambda^2}{9}\right) \exp\left\{-\frac{(b_2^0)^2\left(1 + \frac{\lambda^2}{3}\right)}{2\sigma^2}\right\}$$

($\lambda = b_2^2/b_2^0$) with $\sigma = 0.081$ cm^{-1} and $d = 3$ (20) ($0 \langle b_2^0(cm^{-1}) \langle 0.24$). The XRD spectrum of deposited GaF_3 is typical of amorphous compounds. This compound kept for a few hours at room atmosphere partially crystallizes to an hydrated form GaF_3, $3H_2O$. Heating of the amorphous GaF_3 ($T_X = 293$°C (3)) under dry atmosphere leads to the formation of Rh–GaF_3. EPR and XRD spectra of recrystallized GaF_3:Fe^{3+} are slightly less resolved but very similar to those of Rh–GaF_3:Fe^{3+}. Therefore, the recrystallization of amorphous GaF_3, leads to well-crystallized Rh–GaF_3 from both medium- and short-range order points of view. The system evolves from a distribution of slightly distorted octahedra (parameter distribution with a maximum for $\lambda = 1$ and $b_2^0 = 0.1$ cm^{-1} (20)) to a system composed of regular octahedra (described by a single set of parameters $b_2^0 = 0.019$ cm^{-1} and $\lambda = 0$).

TABLE 5
Ionic Radii (Å) for Sixfold Coordinated Cations and Fluorine Anions

Al^{3+}	Ga^{3+}	In^{3+}	Cr^{3+}	Fe^{3+}	F^-
0.535	0.620	0.800	0.615	0.645	1.285

AMORPHOUS $PbGaF_5$ RECRYSTALLIZATION

As for the amorphous GaF_3:Fe^{3+} EPR spectrum, the $PbGaF_5$:Fe^{3+} EPR spectrum exhibits two main resonances at $g_{eff} = 4.3$ and $g_{eff} = 2.0$ (Fig. 5). The Fe^{3+} EPR spectra of recrystallization compound of amorphous $PbGaF_5$ ($T_X = 283$°C (3)) and crystallized $PbGaF_5$ exhibit resonances located at the same magnetic field values (350, 1500, and 3400 Gauss). Although XRD spectra suggest a similar crystalline state for recrystallized and crystalline $PbGaF_5$ powder, the EPR spectra differ by the resonance relative intensity (Fig. 5). A raw structural determination suggests the existence of three different Ga^{3+} sites (21) which could explain the observed differences in relative intensities (different probe site occupancies). The knowledge of every EPR probe site spectrum would confirm this assumption. The existence of antiferromagnetic pairs of Fe^{3+} ions could be responsible for the high-intensity resonance at $g_{eff} = 2.0$ in the recrystallized compound, as it is in TMFG (20). As observed in the GaF_3 case, the EPR spectrum of the recrystallized compound is less resolved than that of the crystalline compound. All these observations show that recrystallization of $PbGaF_5$ leads to the formation of a compound whose crystalline state, from a local point of view, is not as good as crystalline $PbGaF_5$.

PZG: Cr^{3+} AND Fe^{3+} RECRYSTALLIZATION AT 400°C

EPR spectra of PZG glass ($T_X = 283$°C (22)) doped with both Cr^{3+} and Fe^{3+} ions were studied as a function of heating time treatment (3 hr to 8 days).

1. PZG: Cr^{3+}

When heating time is increased, the most noticeable point is the increase of the intensity of the $g_{eff} = 2.0$ resonance with regard to the intensity of the $g_{eff} = 5.0$ resonance (Fig. 6).

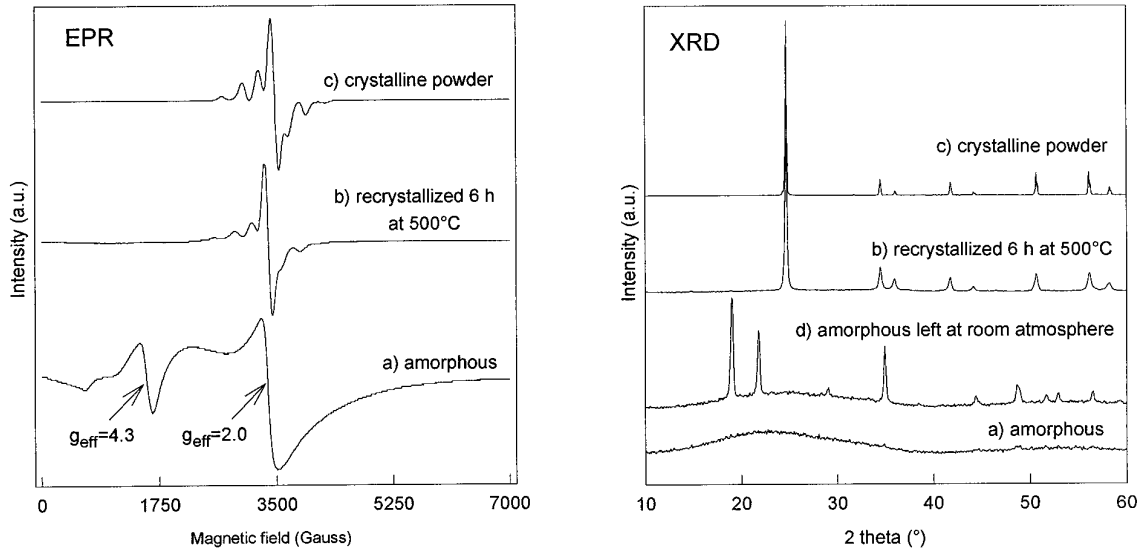

FIG. 4. Fe^{3+} X-band EPR spectra for GaF_3 (a) ν = 9.43 GHz, 2.50 wt% FeF_3, T = 4 K; (b) ν = 9.45 GHz, 1.14 wt% FeF_3, room temperature; (c) ν = 9.66 GHz, 1.0 wt% FeF_3, room temperature and GaF_3 XRD pattern.

After a long heating time, some small broad resonances appear. In order to identify the recrystallization compounds and to attribute these resonances, it is necessary to observe the XRD pattern of the recrystallized glasses. The recrystallization of PZG : Cr^{3+} leads to a mixture of compounds, Pb_2ZnF_6, $Pb_9Ga_2F_{24}$, $PbGaF_5$, and $Pb_3Ga_2F_{12}$. These compounds are easily identifiable owing to their low XRD angles (spectra given in Figs. 7 and 8). The EPR spectra of these compounds doped with CrF_3 (Fig. 9) exhibit a higher intensity ratio $I_{g_{eff}=2.0}/I_{g_{eff}=5.0}$ than glass spectra. It explains the increase of this ratio in EPR glass spectra after heating treatment. The identification of the recrystallization compounds by means of the EPR technique appears rather difficult. The low-intensity resonances of the recrystallized glass spectra could be attributed to $PbGaF_5$ and $Pb_9Ga_2F_{24}$. One can note that the existence of these compounds becomes evident in EPR and XRD spectra after a long heating time. The Pb_2ZnF_6 and $Pb_3Ga_2F_{12}$ resonances do not appear in the EPR spectra whereas their existence is shown by XRD spectra.

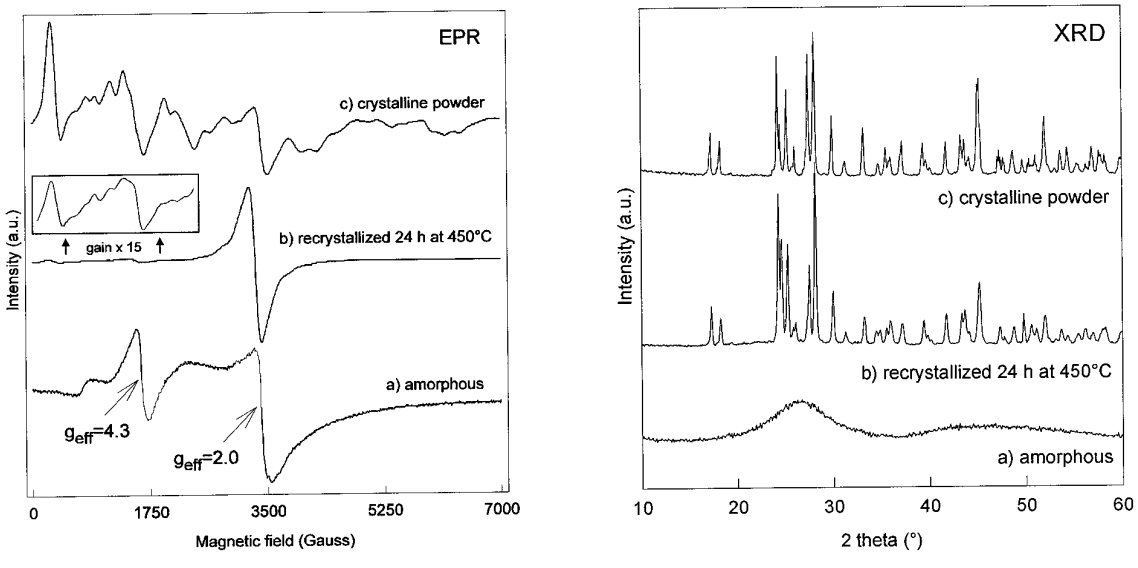

FIG. 5. Fe^{3+} X-band EPR spectra in $PbGaF_5$ (a, b) ν 9.39 GHz, 0.75 wt% FeF_3; (c) ν = 9.38 GHz, 0.60 wt% FeF_3) and $PbGaF_5$ XRD pattern.

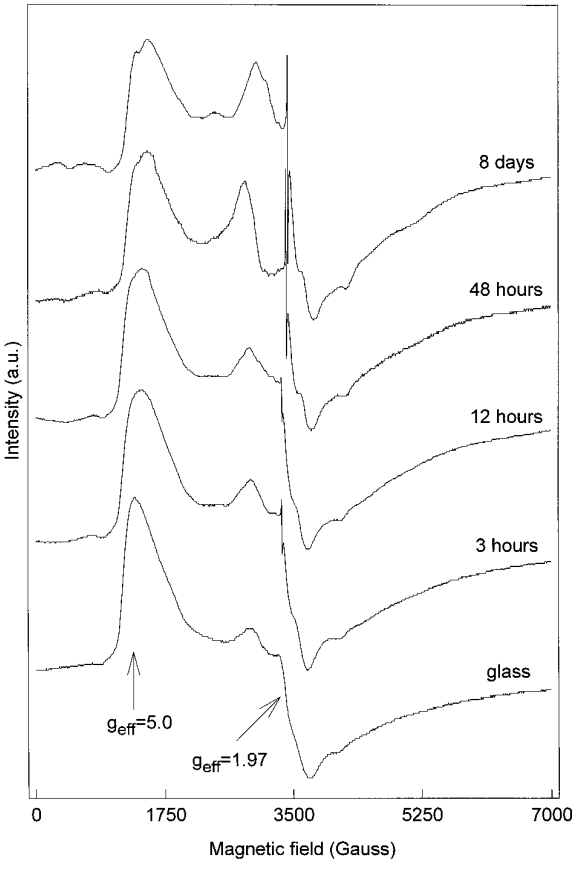

FIG. 6. PZG : Cr^{3+} (1.21 wt% CrF_3) X-band EPR spectra (ν = 9.39 GHz except in the case of glass recrystallized 8 days, for which ν = 9.45 GHz); heating treatment temperature is 400°C.

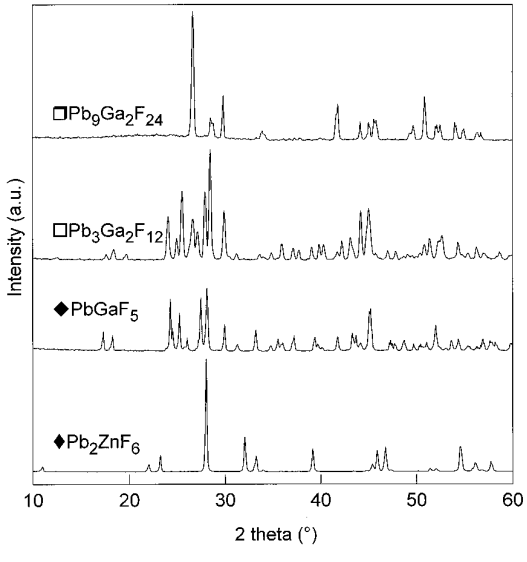

FIG. 7. PZG recrystallization compound XRD pattern.

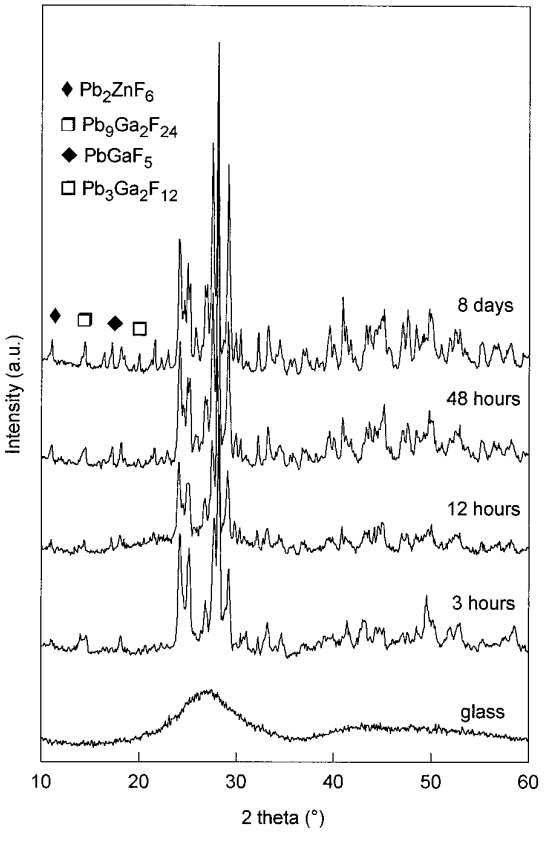

FIG. 8. PZG : Cr^{3+} XRD pattern.

Despite these changes, the Cr^{3+} EPR spectra of PZG glasses remain typical of disordered compounds. If the low-intensity resonances were not considered, these spectra could be simulated with a distribution of fine structure parameters with weaker σ value than for the glass spectrum (a weaker σ value induces weaker b_2^0 values and then an increase of the intensity of $g_{\text{eff}} = 1.97$ resonance is observed when the intensity of the $g_{\text{eff}} = 5.0$ resonance decreases (1)).

In Fig. 6, one can note the appearance of a very sharp feature in the $g = 2$ region, without hyperfine structure, whose amplitude increases with heating time. This effect has been observed once only. The signal is nearly symmetric with $g = 2.0031$ and a linewidth $\Delta H_{\text{pp}} = 1.8$ Gauss. These values are both incompatible with Cr^{5+} ions (23) and radiation-induced defect centers, the ns^1 defect center (Zn^+ or Pb^{3+}), and F-, H-, E′-, and V-type centers (24, 25). It is out of question that this line arises from conduction electrons as its intensity (peak-to-peak height X width^2 for derivative spectrum) increases with decreasing temperature according to paramagnetic Curie law ($\chi = C/T$), which is in agreement with the expectation of a paramagnetic center. This signal is ascribed to a free-like electron carrier species which does not appear at room temperature but

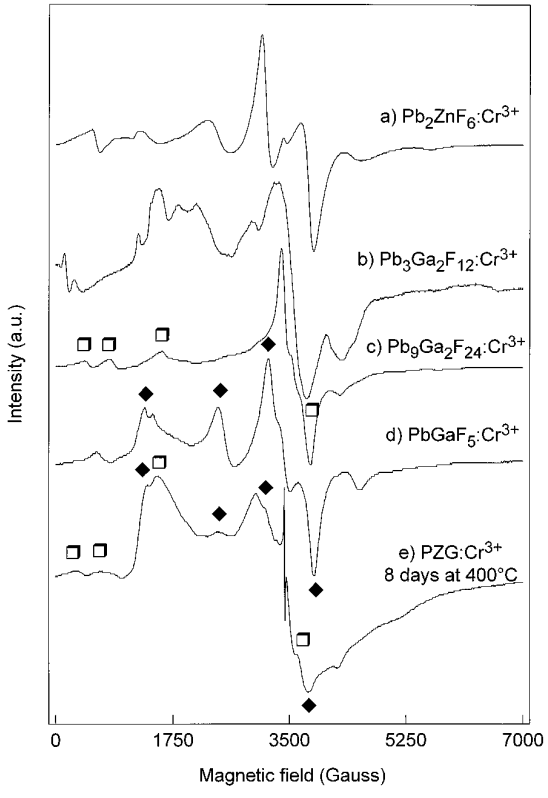

FIG. 9. X-band EPR spectra of Cr^{3+}-doped recrystallized PZG and recrystallization compounds of PZG: (a) 0.61 wt% CrF_3, ν = 9.38 GHz; (b) 0.46 wt% CrF_3, ν = 9.38 GHz; (c) 0.47 wt% CrF_3, 9.73 GHz; (d) 0.58 wt% CrF_3, ν = 9.74 GHz; (e) 1.21 wt% CrF_3, ν = 9.45 GHz.

only when the sample is heated. This electron doesn't interact with the F nucleus (nuclear spin $I = 1/2$). It might be formed from an impurity present in the starting glass. It was found to be stable over several months.

2. PZG: Fe^{3+}

As for Cr^{3+}, the Fe^{3+} EPR spectra of PZG glass are characteristic of disordered compounds after a heating treatment (Fig. 10). After a heating period of three hours, an increase of the intensity ratio $I_{g_{\text{eff}}=2.0}/I_{g_{\text{eff}}=4.3}$ is observed. For longer heating treatment, the intensity ratio increased no more and few resonances appear at low magnetic field values. This resonance identification can be achieved by means of the XRD pattern of the recrystallized PZG : Fe^{3+} (Fig. 11). The XRD pattern of recrystallized PZG : Cr^{3+} and PZG : Fe^{3+} are not similar, although they went through the same heating treatment (simultaneous heating in the same furnace). This clearly shows the influence of the Cr^{3+} and Fe^{3+} ions on the structure of PZG glasses. Although FeF_3 is one of the potential constituents of the glass (GaF_3 can be fully substituted by FeF_3 (22)), the addition of a small amount of CrF_3 induces glass crystallization. For PZG : Fe^{3+}, the $PbGaF_5$ proportion seems to be higher and no trace of $Pb_3Ga_2F_{12}$ is observed. The EPR spectra of the three observed compounds doped with Fe^{3+} are given in Fig. 12. The wide resonances in Fig. 10, appearing at low magnetic field values, can be attributed to $PbGaF_5:Fe^{3+}$. EPR doesn't give evidence for any other compounds in the reheated glasses. This result is coherent with the evolution of the spectra in Fig. 10. The $PbGaF_5:Fe^{3+}$ EPR spectrum is characterized by a low-intensity ratio $I_{g_{\text{eff}}=2.0}/I_{g_{\text{eff}}=4.3}$. Thus, the evolution of this ratio (constant for a heating time longer than three hours) can be explained by the preponderant presence of $PbGaF_5$ for long treatments.

CONCLUSION

Observations of GaF_3 and $PbGaF_5$ behaviors show that the recrystallization of amorphous compounds seems to be related to the degree of symmetry of the corresponding crystallized product; the higher the symmetry, the easier the recrystallization. Furthermore, if the recrystallization

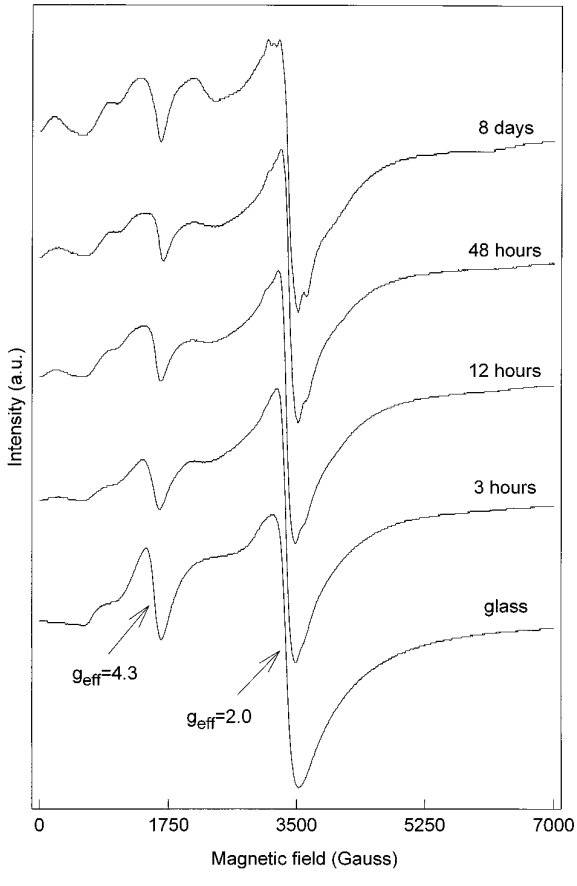

FIG. 10. PZG : Fe^{3+} (1.21 wt% FeF_3) X-band EPR spectra (ν = 9.39 GHz except in the case of glass heated 8 days, for which ν = 9.45 GHz); heat treatment temperature is 400°C.

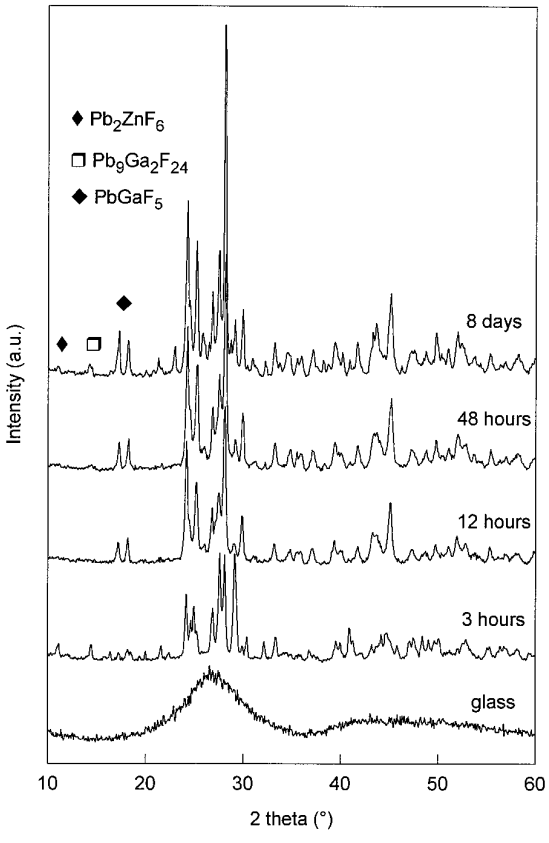

FIG. 11. PZG : Fe^{3+} XRD pattern.

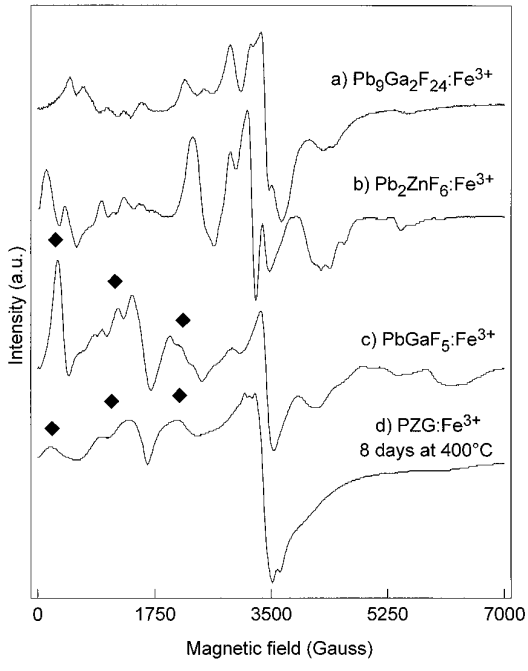

FIG. 12. X-band EPR spectra of Fe^{3+}-doped recrystallized PZG and recrystallization compound of PZG: (a) ν = 9.38 GHz, 0.24 wt% FeF_3; (b) ν = 9.37 GHz, 0.38 wt% FeF_3; (c) ν = 9.45 GHz, 0.57 wt% FeF_3; (d) ν = 9.45 GHz, 1.21 wt% FeF_3.

leads to several compounds, determination of the nature of recrystallized products by means of EPR is difficult as the probe ions may be selectively segregated into only some of the many compounds present in the recrystallized glasses. Therefore the probe-Ga^{3+} substitution seems to be prohibited in some of them. Nothing can easily explain this observation apart from the Pb_2ZnF_6 case (in which there is no 3+ cation).

This study clearly illustrates the difference of sensitivity to short- and medium-range disorder of EPR and XRD techniques. MF_6 octahedra essentially linked by corner are the basic structural units of TMFG and recrystallization compounds. During recrystallization, these structural units rearrange by slight ion motion leading to narrower cation–cation distance distribution; medium-range order is then more affected than local order. Thus, EPR does not appear to be an appropriate technique to investigate recrystallization in PZG glass as local disorder in recrystallized glasses is comparable to the disorder in the starting glasses. This observation confirms the slight distortion found for GaF_6^{3-} constituent octahedra in PZG glass and in amorphous GaF_3 (1). This also explains the successful modelization of TMFG local order with the help of crystalline $CsZnGaF_6$, which is characterized by a statistical distribution of octahedrally coordinated 3*d* ions in the same site leading to a local disorder related to slight displacement of anions (1). Thus it is not surprising to note that Cr^{3+} and Fe^{3+} EPR spectra in $CsZnGaF_6$ and in recrystallized PZG glass are very similar (1).

REFERENCES

1. C. Legein, J. Y. Buzaré, B. Boulard, and C. Jacoboni, *J. Phys. Condens. Matter* **7,** 4829 (1995).
2. C. Jacoboni, A. Le Bail and R. De Pape, *Glass Technol.* **24,** 164 (1983).
3. B. Boulard, A. Le Bail, C. Jacoboni, and J. H. Simmons, *Mater. Sci. Forum* **32–33,** 61 (1988).
4. B. Boulard and C. Jacoboni, *Mater. Res. Bull.* **25,** 671 (1990).
5. J. Chassaing and A. Erb, *C. R. Acad. Sci. Paris C* **t270,** 949 (1970).
6. M. Samouel, *C. R. Acad. Sci. Paris C* **t268,** 409 (1969).
7. P. Daniel, A. Bulou, M. Rousseau, J. Nouet, J. L. Fourquet, M. Leblanc, and R. Burriel, *J. Phys. Condens. Matter* **2,** 5663 (1990).
8. F. M. Brewer, G. Garton, and D. M. L. Goodgame, *J. Inorg. Nuclear Chem.* **9,** 56 (1959).
9. R. Hoppe, and D. Kissel, *J. Fluorine Chem.* **24,** 327 (1984).
10. A. Abragam and B. Bleaney, ''Electron Paramagnetic Resonance of Transition Ions.'' Dover, New York, 1986.
11. P. Daniel, Thesis, University of the Maine, France, 1990.
12. D. J. Newman, *Adv. Phys.* **20,** 197 (1971).
13. S. Houlbert, Thesis, University of Caen, France, 1992.
14. R. D. Shannon, *Acta Crystallogr.* **A32,** 751 (1976).
15. E. A. Harris, *Phys. Chem. Glasses* **28,** 196 (1987).
16. L. D. Bogomolova, F. Caccavale, N. A. Krasil′Nikova, and S. I. Reiman, *J. Non-Cryst. Solids* **91,** 203 (1987).
17. D. L. Griscom and R. J. Ginther, *J. Non-Cryst. Solids* **113,** 146 (1989).

18. C. Legein, J. Y. Buzare, and C. Jacoboni, *J. Non-Cryst. Solids* **161,** 112 (1993).
19. G. Czjzek, J. Fink, F. Götz, H. Schmidt, J. M. D. Coey, J. P. Rebouillat, and A. Lienard, *Phys. Rev. B* **23,** 2513 (1981).
20. C. Legein, J. Y. Buzare, J. Emery, and C. Jacoboni, *J. Phys. Condens. Matter* **7,** 3853 (1995).
21. B. Boulard, Thesis, University of the Maine, France, 1989.
22. J. P. Miranday, C. Jacoboni, and R. de Pape, *J. Non-Cryst. Solids* **43,** 393 (1981).
23. S. A. Al′Tshuler, B. M. Kozyrev, ''Electron Paramagnetic Resonance in Compounds of Transition Elements.'' Wiley/Keter Publishing House, New York/Jerusalem, 1974.
24. D. L. Griscom, *J. Non-Cryst. Solids* **161,** 45 (1993).
25. D. L. Griscom, *J. Non-Cryst. Solids* **40,** 211 (1980).